Key Engineering Materials
ISSN: 1662-9795, Vol. 1049, pp 1-11
doi:10.4028/p-5o49gU

Submitted: 2025-12-11
Revised: 2026-02-11
Accepted: 2026-03-02
Online: 2026-04-15

Advanced Control of Stretch-Reducing Mills Using Artificial Intelligence

Laura Antonini[1,a *], Mariangela Quarto[1,b], Claudio Giardini[1,c], Giuseppe Pellegrini[1,d] and Marco Zambelli[1,e]

[1]Department of Management, Information and Production Engineering, University of Bergamo, Via Pasubio 7/b, 24044 Dalmine, BG, Italy

[a]laura.antonini@unibg.it, [b]mariangela.quarto@unibg.it, [c]claudio.giardini@unibg.it, [d]giuseppe.pellegrini@unibg.it, [e]marco.zambelli@unibg.it

Keywords: Stretch-reducing mill, Artificial Neural Network, Intelligent process control

Abstract. The stretch-reducing mill is a forming process to manufacture tubes by progressive metal deformation. This process is characterized by high complexity and a high number of variables that are strongly interconnected. To overcome the limitations and substantial simplifications of the traditional modelling and offer higher flexibility and suitability for real-time control, an Artificial Neural Networks approach is employed. By defining three parallel networks, they were predicted the milling status, the tube thickness and the angular speeds of the stands composing the process. With the models results, an optimization algorithm is employed to determine the best configuration of angular speeds of the stands to obtain a defined final tube thickness. The Artificial Neural Networks show extremely low RMSE across training, validation, and test sets, confirming their ability to model complex nonlinear dependencies. The optimisation stage reaches the target thickness with only 0.0079% error while preventing unstable operating conditions. The overall methodology provides a tool for implementing the intelligent and data-driven control of the stretch-reducing mill.

Introduction

The stretch-reducing mill (SRM) is a forming process widely applied for producing tubes. The deformation is caused by a sequence of stands whose angular speeds determine the stress distribution along the tube. Due to the complexity of the process, small variation in inter-stand tensions can generate significant effect on stability, potentially leading to slippage or drawing [1].

In a stretch-reducing mill, one of the only manageable variables is the angular speed of the rolling stands (ω). During the process, the material flow rate, resulting from the multiplication between the area and the speed, remains constant due to mass conservation. The speed difference between stands and the tube creates some tensions that can lead to two different limit milling conditions: if the tube moves slower than the maximum tangential stand speed, a slippery condition occurs; if the tube moves faster, the system enters a drawing situation [1]. Another important phenomenon that cannot be ignored is the creep, referring to a viscous deformation occurring under constant load at high temperature [2].

Therefore, the tube thickness decreases in the space between stands, while it increases inside the single stand. This leads to an unpredictable variation of the wall thickness: the process must be carefully monitored and controlled to avoid instability, slippage, or excessive plastic or viscous deformation.

The traditional analytical or numerical models of SRM provide a valuable outcome but often require great simplifications and consider many interdependent variables, requiring high computational power. The variation of the angular speeds (ω) of the stands affects the next ones, creating a cascade effect on the entire process that is difficult to represent and predict with the traditional physical models [3].

In this complex contest, data-driven methods such as Artificial Neural Networks (ANNs) fit particularly well. These models are able to describe the dynamic behaviour of the SRM process, learning hidden relationships among variables while ensuring technological and mechanical consistency. They provide more flexibility in modelling, especially with non-linear and multivariate processes [4]. The applications of Artificial Neural Networks in manufacturing context can enhance

almost real-time and accurate problems detection, enhancing continuous improvement strategies [5]. By optimization algorithms, as the backpropagation [6], they provide systems able to perform intelligent process control and support during the decision-making process.

The main purpose of this work is to present a novel methodology that integrates physics-informed data generation, three parallel ANNs modelling various aspects of SRM process, and an optimization algorithm that computes valid stress distribution to obtain the desired final tube thickness. Differently from other works, the proposed framework perform classification, regression of the thickness and angular speeds predictions, improving robustness near limit situations. The simulation tool adopted in this work is not a finite element but, starting from analytical formulations, it is built a physics-informed simulation tool for data generation. Then, it is developed an ANN-based approach with multiple parallel networks to manage the consecutive rolling stands and their interconnections. The models are evaluated in order to provide accurate predictions and guarantee model adaptability and scalability. Subsequently, an optimization algorithm [6] is applied to support the definition of the best combination of angular speeds (ω) to be set to obtain the desired tube thickness with the minimum error. This approach is designed for high interpretability, physical consistency, and potential real-time deployment.

The Milling Process

The SRM is a forming process composed of a sequence of rolling stands that progressively reduce the tube diameter while adjusting the wall thickness [7]. Since there is no mandrel, deformation in SRM is managed exclusively by kinematics of the stands, which makes the control problem particularly sensitive to distribution of the inter-stands stresses.

In addition to the stands angular speed, there are other forces and parameters to keep into account when analysing a stretch-reducing mill process. The mechanical equilibrium can be described through the balance of stresses in the normal and tangential directions. More in detail, as shown in Fig. 1, R is the roll radius at the point of contact with the material, r represents the radial position of the element within the workpiece, p is the contact pressure exerted by the roll on the material, α represents the angle of contact or inclination between the roll and the material at a given point, dα is the infinitesimal angle swept by the roll in the axial direction (along the arc of contact), dϑ is the infinitesimal angle along the circumferential direction of the material, h represents the thickness of the material at the section under consideration, σ_ϑ is the circumferential stress, σ_a is the axial stress and $d\sigma_a$ is the incremental change in axial stress across the differential element.

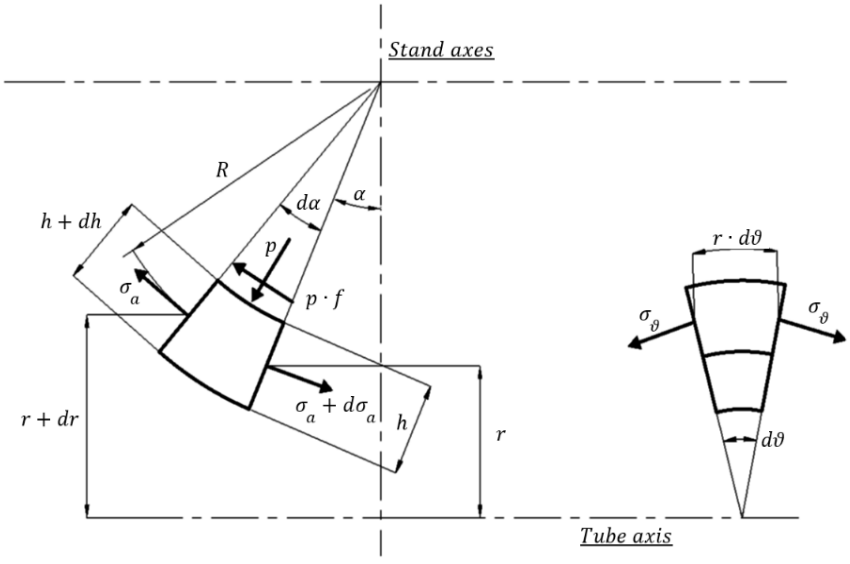

Fig. 1. Stress state representation in the tube.

The balance in the pressure direction can be described in (1):

$$p \cdot R \cdot d\alpha \cdot r \cdot d\vartheta - \sigma_a \cdot h \cdot r \cdot d\vartheta \cdot \sin\frac{d\alpha}{2} - (\sigma_a + d\sigma_a) \cdot h \cdot r \cdot d\vartheta \cdot \sin\frac{d\alpha}{2} + 2\sigma_\vartheta \cdot \sin\frac{d\vartheta}{2} \cdot h \cdot R \cdot d\alpha \cdot \cos\alpha = 0 \quad (1)$$

Given f as the friction coefficient between the roll and the material, dh as the incremental change in thickness of the material, dr as the incremental change in radial position of the differential element, the tangential direction on the meridional plane can be described as in (2):

$$f \cdot p \cdot R \cdot d\alpha \cdot r \cdot d\vartheta + \sigma_a \cdot h \cdot r \cdot d\vartheta \cdot \cos\frac{d\alpha}{2} - (\sigma_a + d\sigma_a)(h + dh)(r + dr) \cdot d\vartheta \cdot \cos\frac{d\alpha}{2} + 2 \cdot \sigma_\vartheta \cdot R \cdot d\alpha \cdot h \cdot \sin\alpha \cdot \frac{d\vartheta}{2} = 0 \quad (2)$$

The plastic deformation condition can be described by the (3), where σ_0 is the equivalent stress of the material:

$$(\sigma_a - \sigma_\vartheta)^2 + (\sigma_\vartheta + p)^2 + (-p - \sigma_a)^2 = 2 \cdot \sigma_0^2 \quad (3)$$

Therefore, considering σ_z as the stress in the axial direction, the stress-strain relationship is reported in (4):

$$\frac{\frac{dh}{h}}{2\sigma_z - \sigma_a - \sigma_\vartheta} = \frac{\frac{dr}{r}}{2\sigma_\vartheta - \sigma_a - \sigma_z} \quad (4)$$

By analysing the behaviour of the function with respect to α, it is possible to identify the neutral section (α_n) in a graphical way as the curve cross (Fig. 2).

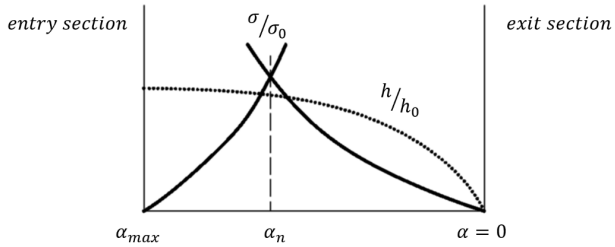

Fig. 2. σ_α distribution in an isolated stand.

Therefore, considering h_0 and r_0 as the thickness and the radius of the material at the entry of the deformation zone, and h_e and r_e as the thickness and the radius of the material at exit section in the deformation zone, the final thickness value results as:

$$h_e = h_0 \sqrt{\frac{r_0}{r_e}} \quad (5)$$

These set of equations represent the tube thickness evolution along the milling process. It is important to also consider the creep phenomenon as its influence corresponds to a thickness reduction.

Finally, considering that the volumetric flow rate of the tube that must be constant, given by the multiplication between the area and the speed, it possible to determine the angular speed of each stand ω_i.

In practice, these relationships can be employed to define a certain axial stress distribution between the stands to derive the thickness variation and identify possible boundary conditions (drawing and slipping) due to a too high inter-stand tension.

The framework described represents the foundation for generating the data employed in the neural networks presented in the following sections.

Methodology

Framework overview

The dataset employed in this work was generated through a simulation pipeline based on the mechanical and technological characteristics of the milling process. It included the infeed and outfeed thickness of each stand, along with the dimensional setup of each stand. Based on this configuration, they were calculated the infeed and outfeed thickness of the tube at each stand. After the generation of the dedicated dataset, the entire developed neural networks were applied to it to simulate and evaluate the rolling process behaviour.

At the end, an optimisation algorithm was applied to determine the best inter-stand tension values, by minimizing the error between the target and the predicted final tube thickness.
The overall workflow is reported in Fig. 3.

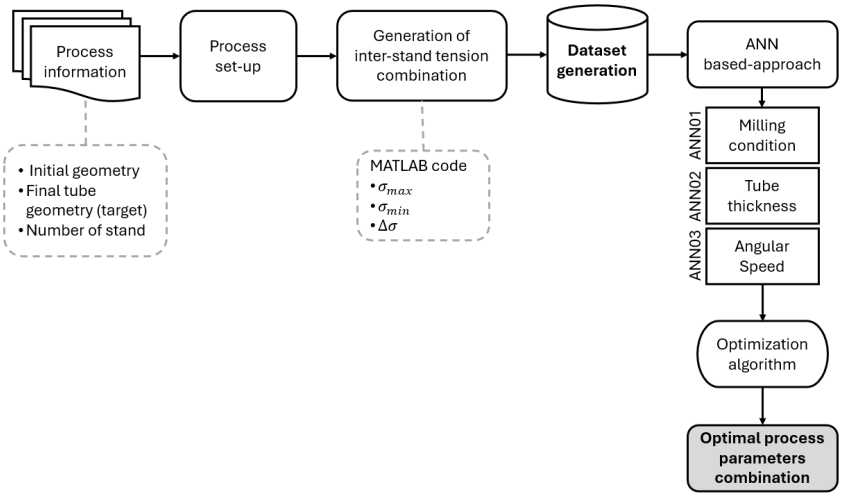

Fig. 3. Study workflow.

Data generation

The dataset employed in this work was designed following the physical characteristics of the stretch-reducing milling process. It was defined a physics-based data generator derived from established analytical formulations of SRM process. Although the data were simulated, this study allowed to analyse the milling operating situations. The numerical model did not have the goal to outperform the state-of-the-art finite element model, but it was designed to generate training data for real-time control. A structured pipeline was defined in MATLAB®R2024b.

Starting from the first phase, it was created a configuration file reporting the dimensional properties of the process including the characteristics of the system (number of stands, etc.), the tube initial diameter, and the material (temperature, creep behaviour, etc). Then, all the feasible combinations of inter-stand stresses were generated with a loop search the entire stress range, specifying the maximum and minimum value of these stresses (σ_{min}, σ_{max}) and the step size ($\Delta\sigma$). These parameters were selected based on the specific analysis to limit high stress between stands that could damage or even rupture the tube. They ensured physical conditions while excluding excessive tensions. Therefore, slippage and drawing conditions were excluded to ensure only realistic combinations. Each combination was used as input into the simulation tool that computes the evolution of process variables during the process. For each combination, it was calculated also the angular speed of all the stands (ω_i), the infeed and outfeed thicknesses of the tube, and the state of each stand (slippage or drawing). Simulations for which the physical conditions were not followed were filtered out to keep the data quality.
In the end data were extracted and formatted to create the final dataset counting around 2600 parameters combinations and containing: inter-stand tensions, the state of the stands as categorical values (0 as the acceptable situation, 0.5 as slippage, 1 as drawing), the computed angular speeds (ω_i),

the infeed tube thickness for each stand, and the final outfeed thickness at the end of the whole process.

From this dataset, the ANNs could learn the hidden relationships between variables ensuring high generalization capabilities.

Artificial Neural Networks

The main purpose of the work is the optimization of the stress distribution between the stands of the stretch-reducing mill to achieve the desired final thickness of the rolled material. Three artificial neural networks (ANN) were developed in cascade to simulate the process behaviour, while an iterative optimisation strategy was employed to find the best inter-stand tension values.

The networks were developed through the use of Python programming language and the PyTorch libraries. Data were scaled using the Min-Max normalization ranging from zero to one. All the networks took as input the inter-stand tensions obtained by physical-based simulation. The networks had the same activation function: tangent sigmoid for the hidden layer, while a pure linear function was applied in the output layer. It was split into 70% for training, 15% for validation, and 15% for testing in each network. As optimizer it was selected the L-BFGS (Limited-memory Broyden–Fletcher–Goldfarb–Shanno) [6] due to its suitability to small-to-medium sized networks and with limited data availability. Following a hyper parametrization process, the learning rate, which explains how quickly a machine learning model updates its parameters during training, was set to 0.5, a high value mitigated by the optimizer. The maximum iterations were defined as 500 and the history size as 10.

As anticipated, three ANNs were designed to model the stretch-reducing mill process.

The first network was used to predict the milling condition ($status_{1\text{-}6}$) where values close to zero were considered acceptable, close to 1 for drawing or close to 0.5 for slippage. The inputs were the inter-stand tensions ($T_{1;2}$, $T_{2;3}$, $T_{3;4}$, etc.). To balance model simplicity and performance, the network configuration was a feedforward net with 15 neurons in the hidden layer. The network scheme is represented in Fig. 4, where on the left are reported inputs, net and outputs, while on the right are shown the specifications with the representation of the activation functions.

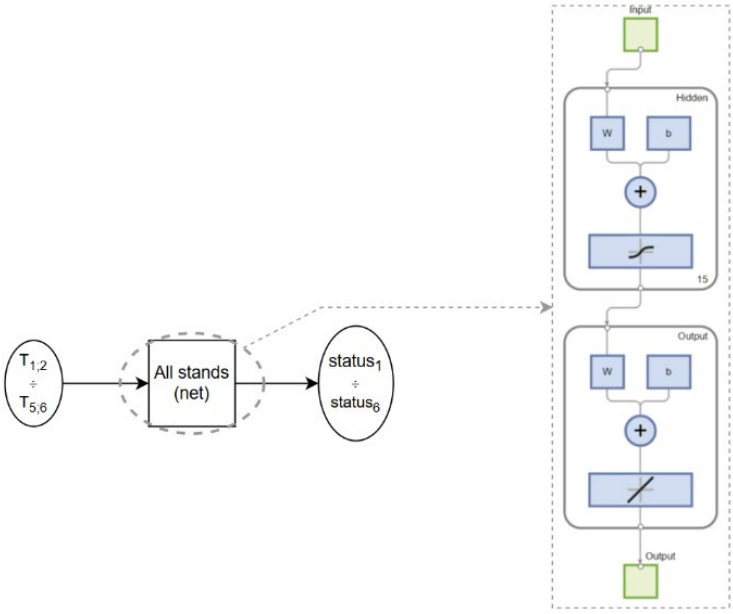

Fig. 4. First network: tensions to status.

The second one employed (Fig. 5) the inter-stand tensions ($T_{1;2}$, $T_{2;3}$, $T_{3;4}$, etc.) to predict the tube thicknesses (t_2, t_3, t_4, etc.). The hidden layer dimension was defined as 15 neurons based on the same reasoning as for the first net. To reflect the real behaviour of the milling process, the network was composed by 6 sub-nets, one for each stand, which use the output of the previous net as part of the

input layer. The first stand received as input the initial tube thickness (t_0), the first inter-stand tension ($T_{1;2}$) and predict the tube thickness (t_1) after the first stand. This predicted value, along with the previous and the subsequent tensions, became the input for the second sub-net, and so on. The last sub-net received as input only the previously predicted thickness and the previous tensions, and it predicted the final tube thickness (t_f). Additionally, each sub-net took into account also the creep effect between stands.

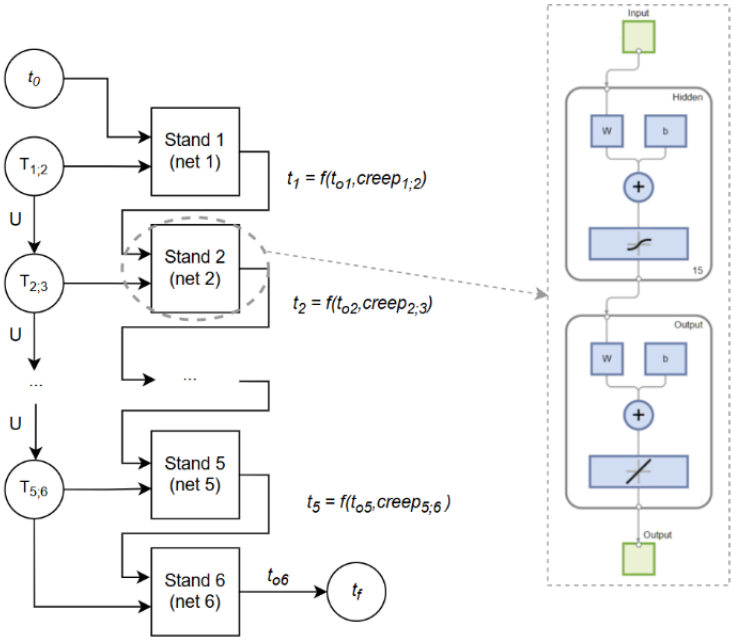

Fig. 5. Second network: tensions to thickness.

The third network (Fig. 6) took as input the inter-tensions ($T_{1;2}$, $T_{2;3}$, $T_{3;4}$, etc.) to forecast the angular speeds ($\omega_{1\text{-}6}$) of the stands. Always considering the balance between performance and task complexity, the hidden layer was defined as 10 neurons. The angular speeds are derived considering one stand speed as fixed reference, typically set to 1, and expressing all other stand speeds relatively to it. This reflects a physical constraint of the process, where only one stand's speed is physically fixed, and the others are adjusted accordingly. Each stand is represented by a single network that predict the corresponding angular speed (ω_n).

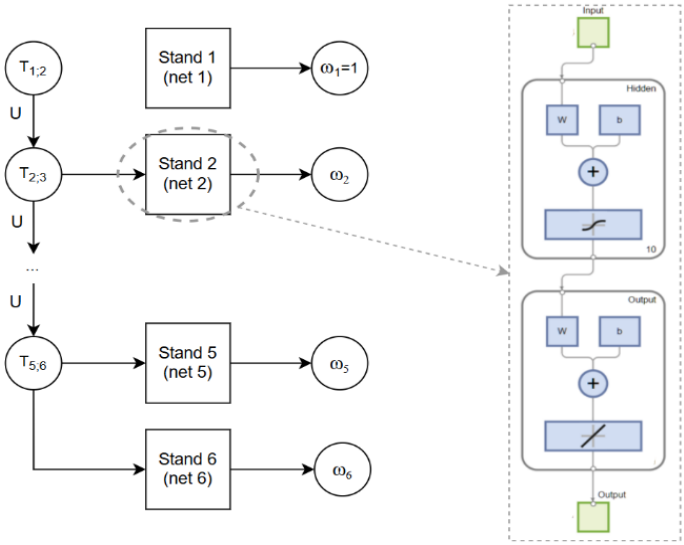

Fig. 6. Third network: tensions to angular speeds.

To evaluate the performance of the ANN, several well-known indices were computed. The network loss was defined as the Mean Squared Error (MSE) that quantifies the average squared difference between the predicted and target values. Based on MSE, the Root Mean Squared Error (RMSE) was also calculated together with the Pearson Coefficient (R) to assess the linear correlation between the predicted and actual values.

Optimization algorithm

On the neural networks results it was applied the bisection algorithm [6] to optimize the stress between stands to minimize the predicted and the target final thickness (t_f) of the rolled material. The use of a single scaling factor ensured stability and physical consistency, while limiting the flexibility of the optimization.

The algorithm iteratively searched for the optimal set of inter-stand tensions and therefore of angular speeds. The bisection algorithm is employed to find the root of an equation of the form $f(x) = 0$, when the function is continuous over an interval $[a, b]$ and changes sign at the extremes, hence $f(a) \cdot f(b) < 0$ [6]. According to the Intermediate Value Theorem [8], if a continuous function changes the sign in the interval, at least one solution exists in that interval. The algorithm is based on this principle to progressively narrow the interval until the root is located with the desired precision. Instead of optimising every tensor singularly, the algorithm introduces a scale parameter φ that multiplies the maximum allowed values for each stand, collecting the values in the vector $ub = [T_{max,1}, T_{max,2}, ...]$. In this way the vector of the maximum tension is defined as $x = \varphi * ub$, reducing the problem to a single variable. At the beginning φ was set equal to 0.5, and the algorithm modify φ at each iteration to minimize the objective function. The optimization continues until the absolute error falls below a certain defined threshold of 0.001. With a penalty mechanism, non-physical plausible solutions are discarded: if the absolute maximum of the status exceeds 0.3, a penalty term of 1.000 was included into the objective function.

In this case study the objective function was defined as minimum of the absolute values of the difference between the estimated thickness and the target one:

$$objf = \min | target\_thickness - estimated\_thickness(x) | \quad (6)$$

This simple but effective optimization algorithm ensures stable and controlled convergence to a near-optimal solution within a limited number of iterations.

Case study presentation

In this work it was analysed a 6 stands SRM by using three Artificial Neural Networks. The dataset of these 6 stands milling process was generated following the workflow presented above. The inter-stand tensions related to this case study were 5 ($T_{1;2}$, $T_{2;3}$, $T_{3;4}$, $T_{4;5}$, $T_{5;6}$). The exit thickness of each stand serves as the entry thickness for the following stand (t_1, t_2, t_3, t_4, t_5). The variable references are reported in Table 1.

Table 1. Variables references.

Inter-stand tensions	Stand statuses	Stand angular speeds	Tube thickness entering the stand	Final tube thickness
$T_{1;2}$, $T_{2;3}$, $T_{3;4}$, $T_{4;5}$, $T_{5;6}$	$S_1, \dots, S_6$	$\omega_1, \dots, \omega_6$	$t_1, \dots, t_5$	t_6

By employing the inter-stand tensions as input, the three neural networks predicted the milling status (drawing, slippage or accepted), the final tube thickness and the angular speed of the stands. Then, the metrics were calculated to evaluate the model performance, and it was applied the optimization algorithm to define the best combination of angular speeds to set to obtain the desired final tube thickness.

Results

In order to evaluate the neural networks, they were computed the MSE, RMSE and R values.

The first network was employed to predict the milling status (acceptable, slippage or drawing) starting from the inter-stand tensions. Looking at Fig. 7 and Fig. 8 it is possible to notice that almost all the values are arranged almost perfectly along the bisector line, indicating a strong correspondence between the predicted and the real values. The R coefficients are close to one, confirmed also by the distribution of the values along the line. The analysis stand by stand shows a coherent behaviour with all the stands following the same trend. Table 2 shows the high precision of first network predictions reporting uniformly low MSE and RMSE values across all data. This consistency indicates that the ANN successfully learns the physical thresholds that identify different milling states (acceptable, slippage and drawing), despite of the inherent nonlinearities of SRM kinematics.

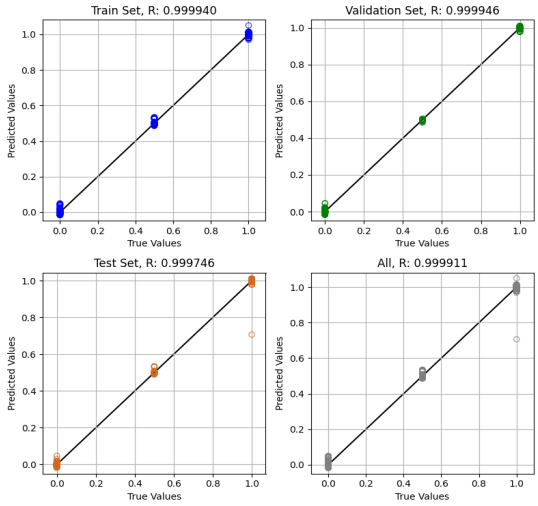

Fig. 7. First network: from inter-stand tensions to the mill status of a mill with 6 stands.

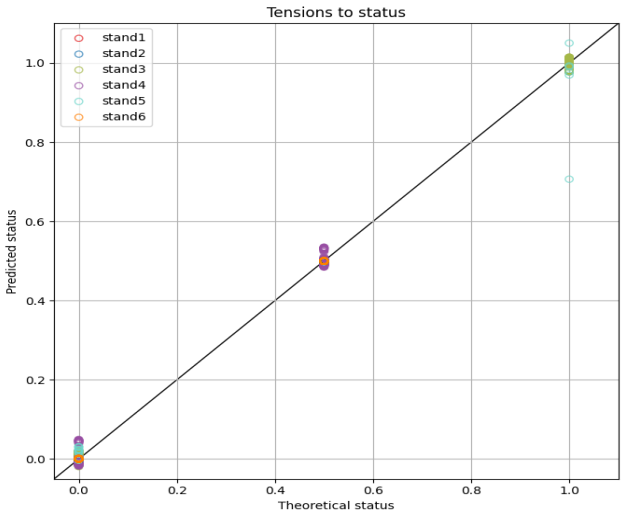

Fig. 8. First network: performance across the different 6 stands.

Table 2. First network performance.

Net 1	All		Training		Validation		Testing	
	MSE	RMSE	MSE	RMSE	MSE	RMSE	MSE	RMSE
	$1.5 \cdot 10^{-5}$	$3.90 \cdot 10^{-3}$	$1.0 \cdot 10^{-5}$	$3.21 \cdot 10^{-3}$	$9.0 \cdot 10^{-6}$	$2.99 \cdot 10^{-3}$	$4.5 \cdot 10^{-5}$	$6.67 \cdot 10^{-3}$

The second ANN used the inter-stand tensions to predict the tube thickness, with a recurrent component to simulate the intermediate tube thicknesses. In Fig. 9, the four scatterplots report a good overlap between the predicted and the actual values. Each stand follows the same tendency without deviations or outliers (Fig. 10). The complexity of thickness predictions arises from non-linear relationships among tensions and parameters across stands. The model reaches a MSE so small to be approximated to zero, while the RMSE values demonstrate high level of precision in prediction (Table 3). The near-net zero RMSE highlights the ability of the ANN to reproduce the complex mechanisms that manage thickness evolution in multi-stands SRM. The network is able to implicitly understand the relationships between parameters and constraints. In addition, the absence of outliers suggests that the network learned to predict thickness as a distributed phenomena and not at a stand-by-stand effect.

This level of accuracy confirms the suitability of the ANN for modelling the behaviour that usually require high computational effort. This level of accuracy allows for reliable integration of the model into control and optimization routines, where small prediction errors translate directly into more stable and physically achievable operating points.

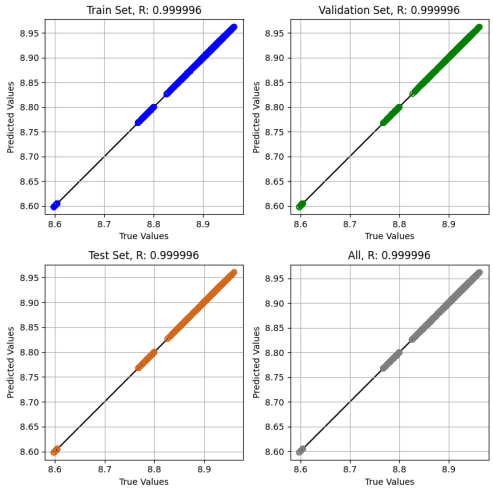

Fig. 9. Second network: from inter-stand tensions to tube thickness.

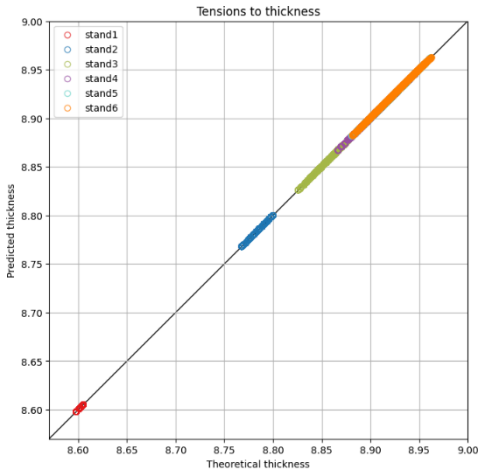

Fig. 10. Second network: performance across the different 6 stands.

Table 3. Second network performance.

Net 2	All		Training		Validation		Testing	
	MSE	RMSE	MSE	RMSE	MSE	RMSE	MSE	RMSE
	0	$3.25 \cdot 10^{-4}$	0	$3.24 \cdot 10^{-4}$	0	$3.28 \cdot 10^{-4}$	0	$3.27 \cdot 10^{-4}$

The third network aimed to predict the angular speeds from the inter-stand tensions. The R coefficients are all close to one (Fig. 11), demonstrating that the network is able to learn the relationship between the inter-stand tensions and the angular speeds. The stand analysis presents data that are distributed along the bisector line, without deviations (Fig. 12). The MSE and RMSE values highlighted the model accuracy confirming that the ANN is able to describing the nonlinear kinematic interactions that manage speed adjustments along the SRM (Table 4). Since the angular speed is the main controllable variable in a real SRM system, this level of accuracy if essential. Given the level of accuracy of the predictions obtained, it is possible to define feasible and well-balanced speed settings during optimization, improving process stability.

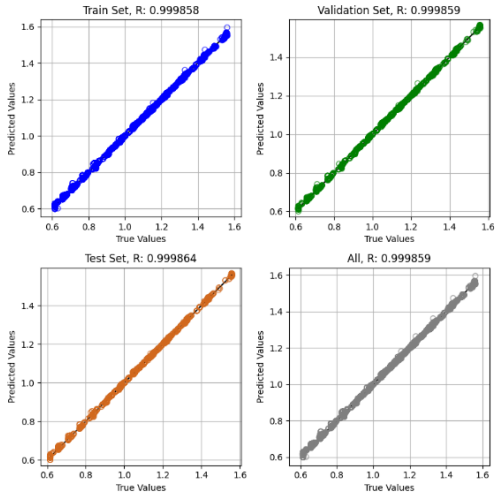

Fig. 11. Third network: from inter-stand tensions to angular speed.

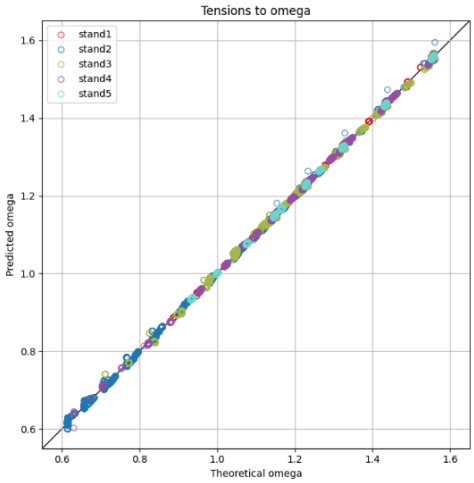

Fig. 12. Third network: performance across the different 6 stands.

Table 4. Third network performance.

Net 3	All		Training		Validation		Testing	
	MSE	RMSE	MSE	RMSE	MSE	RMSE	MSE	RMSE
	$1.3 \cdot 10^{-5}$	$3.56 \cdot 10^{-3}$	$1.3 \cdot 10^{-5}$	$3.58 \cdot 10^{-3}$	$1.3 \cdot 10^{-5}$	$3.57 \cdot 10^{-3}$	$1.2 \cdot 10^{-5}$	$3.48 \cdot 10^{-3}$

Overall, the results obtained across the ANNs demonstrate the ability of the proposed methodology to accurately reproduce the complex interactions managing the SRM behaviour. The low RMSE values and the strong linear fit with the target data (in all ANNs) are particularly significant. In practical, even small deviations in thickness, angular speed, or milling state can spread along the stand sequence and compromise process stability. Therefore, the resulting predictive stability has a direct physical relevance. The results obtained confirm that physical complexity does not always involve model complexity. The achieved accuracy therefore provides a reliable basis for downstream optimization, enabling the definition of physically consistent tension and velocity settings, which would be difficult to achieve using traditional analytical models alone.

When all the process parameters data were predicted, it was applied the bisection algorithm to optimize the process by identifying the optimal set of inter-stand tensions to set in the process to obtain the desired final thickness. As described above, the objective function was defined as the minimum of the absolute value of difference between the target and the predicted thickness values (Eq. 6), ensuring feasibility and accuracy. A penalty was introduced in order to filter out the solutions associated with slippage or drawing.

By analysing the results (Table 5), the optimal solution identified returned a small error of 0.0079%, demonstrating the method accuracy. From the figure (Fig. 13) it is better understandable that the tensions follow a symmetric distribution, avoiding any big value differences that could tear off or damage the tube. The angular speed showed a coherent adaptation, offsetting the effect of the tensions. The status values indicated acceptable milling condition. These results showed that the optimization achieved convergence while preserving realistic milling conditions.

Table 5. Process parameters optimized with the optimization applied on a 6 stands stretch-reducing mill.

	Stand1	Stand2	Stand3	Stand4	Stand5	Stand6
Tensions		0.9	2.8	7.5	2.8	0.9
Status	0.000	0.000	0.0001	-0.000	-0.019	0.290
Angular speed	1.000	0.988	0.888	1.120	1.070	1.132
Thickness	8.605	8.794	8.873	8.932	8.948	8.949

Calculated thickness	8.949
Desired thickness	8.950
Error	$7.08 \cdot 10^{-4}$

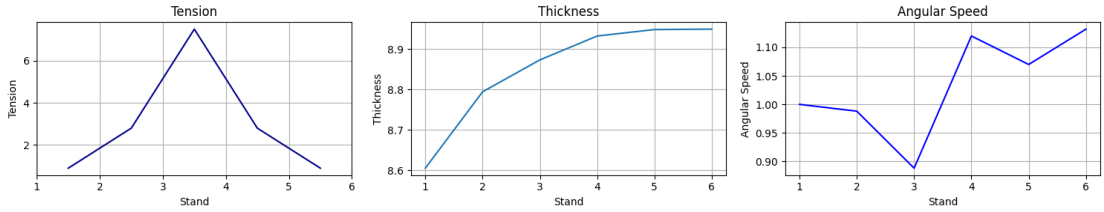

Fig. 13. Optimization results for a 6 stands stretch-reducing mill.

The three ANNs integrated with the optimization algorithm demonstrated high predictive accuracy while maintaining physical feasibility, confirming their suitability for this modelling this process. The observed consistency between training, validation, and testing performance across all ANNs indicates that the developed methodology generalises well beyond the data seen during training. This behaviour is supported by the structure of the dataset, which covers a wide range of feasible tension set, including boundary configurations (close to slippage or drawing). The lack of discrepancy between validation and test errors suggests that there is no overfitting, and that the ANNs remain robust even in regions of the domain that are physically critical or less frequently sampled. This level of generalisation is essential for ensuring reliable use of the models within optimisation-based control strategies.

The obtained results are consistent across stands and predictions, highlighting the capability of the network to understand complex milling relationships. More in detail, the robustness in near limit conditions suggests that the models learned to capture physical feasibility limits. This aspect is crucial to allow operators to understand when a process is going out of control before it actually happens.

Conclusions

The present paper proposed an ANN-based modelling and optimization for stretch-reducing mill validated on physic-informed data. Three parallel neural networks were computed and demonstrated accuracy in predicting the milling status, the tube thickness, and the angular speeds of the stands. The integration of three specific ANNs with an optimization algorithm is able to identify setpoints that are physically feasible, and to reach the desired thickness with a minimal error. The methodology shows a powerfulness in supporting the decision-making process for the intelligent control of the milling process, and it can be extended to real-time supervisory systems, multi-objectives control and predictive quality. The strong generalization capability of the ANNs, underlined by the consistency of training, validation and tests errors, confirms the reliability and efficiency of the developed methodology. By combining physics-informed data generation with accurate data-driven prediction, the proposed methodology represents a promising candidate for next-generation intelligent forming process control. This study is based on simulated data, but experimental validation and multi-parameter optimization remain open directions for future studies in which the proposed framework could be integrated.

References

[1] V. B. Ginzburg, “Steel-Rolling Technology,” 1989. doi: 10.1201/9781466593510.

[2] C. Giardini, A. Bugini, and G. Pellegrini, “Creep Influence in a Stretch Reducing Mill Computer Simulation,” in Proceedings of the Twenty-eighth International, London: Macmillan Education UK, 1990, pp. 455–460. doi: 10.1007/978-1-349-10890-9_62.

[3] A. Ojeda-López, M. Botana-Galvín, L. González-Rovira, and F. J. Botana, “Numerical Simulation as a Tool for the Study, Development, and Optimization of Rolling Processes: A Review,” Metals (Basel), vol. 14, no. 7, p. 737, Jun. 2024, doi: 10.3390/met14070737.

[4] E. Öznergiz, C. Özsoy, I. I. Delice, and A. Kural, “Comparison of empirical and neural network hot-rolling process models,” Proc Inst Mech Eng B J Eng Manuf, vol. 223, no. 3, pp. 305–312, Mar. 2009, doi: 10.1243/09544054JEM1290.

[5] B. Ördek, Y. Borgianni, and E. Coatanea, “Machine learning-supported manufacturing: a review and directions for future research,” Prod Manuf Res, vol. 12, no. 1, Dec. 2024, doi: 10.1080/21693277.2024.2326526.

[6] M. J. Kochenderfer and T. A. Wheeler, Algorithms for Optimization, Second edition. 2019. Accessed: Dec. 11, 2025. ISBN: 9780262039420. Available: https://mitpress.mit.edu/9780262039420/algorithms-for-optimization/

[7] G. Pellegrini, C. Giardini, and A. Bugini, “An Automatic Speed Programme Generation for SRM,” in Proceedings of the Thirtieth International MATADOR Conference, London: Macmillan Education UK, 1993, pp. 211–216. doi: 10.1007/978-1-349-13255-3_28.

[8] M.N. Vrahatis, “Generalization of the Bolzano theorem for simplices,” Topol Appl, vol. 202, pp. 40–46, Apr. 2016, doi: 10.1016/j.topol.2015.12.066.